

**Electronic Supplementary Information
Enantiospecificity in Achiral Zeolites for Asymmetric
Catalysis**

Tianxiang Chen, Sarah J. Day, Chiu C. Tang, Tsz Woon Benedict Lo *

*Correspondence email: benedict.tw.lo@polyu.edu.hk

Supporting information:

1. Materials and Methods

Materials

H-ZSM-5(**MFI**) and H-MOR(**MOR**)

Commercial H-ZSM-5 ($\text{SiO}_2:\text{Al}_2\text{O}_3 = 46$) and H-MOR ($\text{SiO}_2:\text{Al}_2\text{O}_3 = 25$) samples were purchased from Nankai University Catalyst Co., Ltd. Both samples have high crystallinity ($(\geq 95\%)$). Typical characterisation results are displayed on their product website:

[<http://www.nkcatalyst.com/index.php/en/arc/show/id/49.html>]

Cu-exchanged **MFI**

Cu-**MFI** was synthesised via a conventional ion-exchange approach. 1 g H-ZSM-5 ($\text{SiO}_2:\text{Al}_2\text{O}_3 = 46$) was exchanged with 250 mL of 0.01 M copper(II) nitrate hemi(pentahydrate) ($\text{Cu}(\text{NO}_3)_2 \cdot 2.5\text{H}_2\text{O}$) solution for 24 h at 80 °C upon washed and collected for overnight in an oven at 60 °C after drying.

Lysine adsorption

L-lysine hydrochloride (Aldrich 98%) and D-lysine (Aldrich 98%) were used as the lysine source. The pristine zeolite and Cu-**MFI** samples were first suspended in deionized water, L-lysine(L-Lys) and D-lysine(D-Lys) were added, respectively. Then, the solution was stirred for 1 h in room temperature upon washed and collected after drying for overnight in an oven at 60 °C.

Methods

High-resolution synchrotron X-ray powder diffraction (SXRD) and Rietveld refinement

SXRD measurements for *in situ* desorption study were collected at beamline BL02B2 at SPring-8, Japan. The energy of the incident X-ray flux was set at 18 keV¹. The wavelength and the 2θ-zero point were calibrated using a diffraction pattern obtained from a high-quality CeO₂ powder (NIST SRM674b). High-throughput SXRD data were obtained from the zeolite samples (loaded in 0.5-mm borosilicate capillaries) using the Microstrip sYstem for Time rEsolved experimeNts (MYTHEN) detectors, with a modular system constructed by six MYTHEN detectors. The patterns were collected in the 2θ range 2-78° with 0.006° data binning. Each SXRD pattern was collected for 5 min for each 2θ-step, i.e., 10 min in total for MYTHEN data summation. This procedure produced good quality patterns of high signal-to-noise ratio. It should be particularly noted that the R-factors using the MYTHEN detectors are artificially high. Therefore, the quality of the Rietveld refinement should be judged by the difference between the fitted and observed data.

For *in situ* desorption measurements, the samples were heated using a hot N₂-hot air blower at a ramping rate of 10 °C per min. Sequential SXRD measurements were collected at every 25 °C temperature step. The patterns were collected in the 2θ range 2-78° with 0.006° data binning. Each SXRD pattern was collected for 2 min.

Using the TOPAS software, the lattice and structural parameters were obtained using Le Bail and Rietveld refinement analyses of the diffraction patterns. The starting coordinates used were based on the H-ZSM-5 zeolite model by Heo *et al.* for the refinement². The background curve was fitted by a Chebyshev polynomial with an average of 20 coefficients. The Thompson-Cox-Hastings (pseudo-Voigt) function was applied to describe the diffraction peaks³. The scale factor and lattice parameters were allowed to vary for all the histograms. The final refined structural parameters for each data histogram were carried out using the Rietveld method with the fractional coordinates (x, y, z) and isotropic displacement factors (B_{eq}) for all atoms. In addition, the R_{wp} and R_{exp} values are helpful to assess the quality of fit.

(i) Framework atoms

In principle, upon organic molecule adsorption, the positions of the framework atoms may change slightly – a small deviation from the model by Heo *et al.* Therefore, prior to the refinement of the entire structure with lysine molecules, the Si-Al-O atoms of the host framework were first refined, to avoid a miscalculation of the structure that reaches the global minimum. As the guest molecules that were used do not consist of any heavy atoms, it is reasonable to assume these only minimally contribute to the diffracted intensities at low 2θ reflections. Thus, the fractional coordinates and the B_{eq} values of the framework atoms (Si and O) were fixed and all other parameters were refined over the 2θ range of 3-55°.

(ii) Fourier analysis

Over the 2θ refinement range, the Fourier analysis was used to identify the locations with the highest remaining electron density in the framework, once the positions of the most atoms have been determined.

(iii) Inclusion of guest molecules

From the result of the Fourier analysis, a Monte Carlo-based simulated annealing technique was used to locate their positions in the H-ZSM-5. In the simulation, the guest lysine molecules were treated as rigid body of Z-matrices. These were refined, while keeping the fractional coordinates of the framework atoms fixed.

The H-ZSM-5 pre-adsorbed with L/D-lysine samples were refined using two rigid body Z-matrices describing lysine at fixed bond distances and angles, it was first applied to be simulated annealed using the Rietveld method. Thus, the simulated annealing technique ensures the correct number of lysine adsorption sites.

After identifying, the number and location of the adsorption sites, the site occupancy factors (SOFs) were refined. Also, the dihedral angles of the rigid-bodies were refined with restraining to $\pm 10\%$ from the optimised L-/D-lysine structures using Chem3D software. Then, the relevant parameters were relaxed and refined repeatedly for an hour to ensure the global minimum has been reached. The global minimum is indicated by the lowest R_{wp} and gof values.

However, in some cases, the derived crystal structures were not sensible, e.g. the guest molecules are located far too close to the framework – this required a closer check of the parameters before repeating the refinement procedure. Ultimately, several criteria must be met to ensure the high quality and reliability of the refinement, namely, (i) the global minimum has been reached, (ii) the derived crystal structure fits chemical sense, (iii) reasonable systematic error values for all the refined parameters, and (iv) sensible SOF and B_{eq} (temperature or Debye-Waller factor) values.

The temperature factors were constrained in the following way: (i) all the T-sites ($T = Al, Si$) share the same value, and the values for the O-sites are twice the B_{eq} for the T-sites, and (ii) the B_{eq} of the extra-framework atoms were all sensibly fixed at 10 \AA^2 (as B_{eq} is broadly accepted to be about proportional to measurement temperature as that of T-sites)^{4–8}. The atomic and crystallographic parameters are summarized in Tables S4–S6. The position errors of lysine were estimated from the percentage errors of the translation and rotation axes of the rigid bodies.

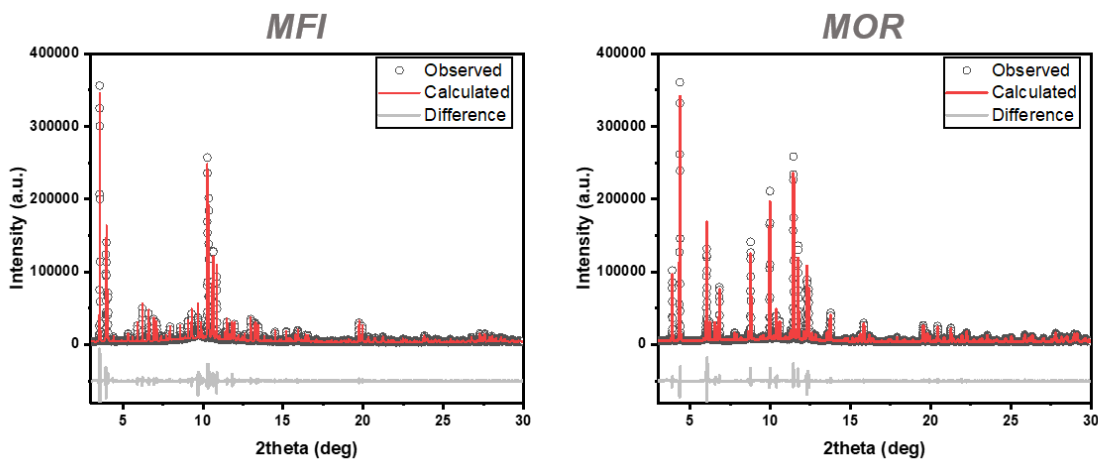


Figure S1. SXRD and Rietveld refinements of pristine **MFI** and **MOR**. The structural parameters are summarized in Table S1.

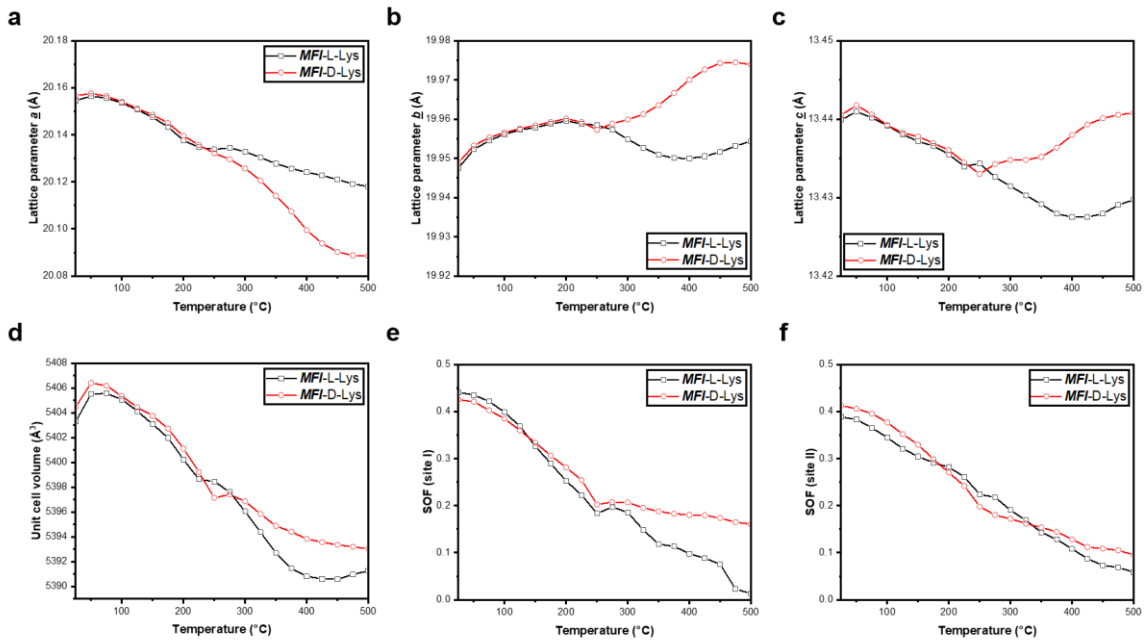


Figure S2. The variation in the structural and atomic parameters from the *in-situ* temperature-programmed desorption SXRD measurements of **MFI-L-Lys** and **MFI-D-Lys**. **(a)** Lattice parameter a , **(b)** lattice parameter b , **(c)** lattice parameter c , **(d)** unit cell volume, site occupancy factors (SOFs) of **(e)** Site I and **(f)** Site II.

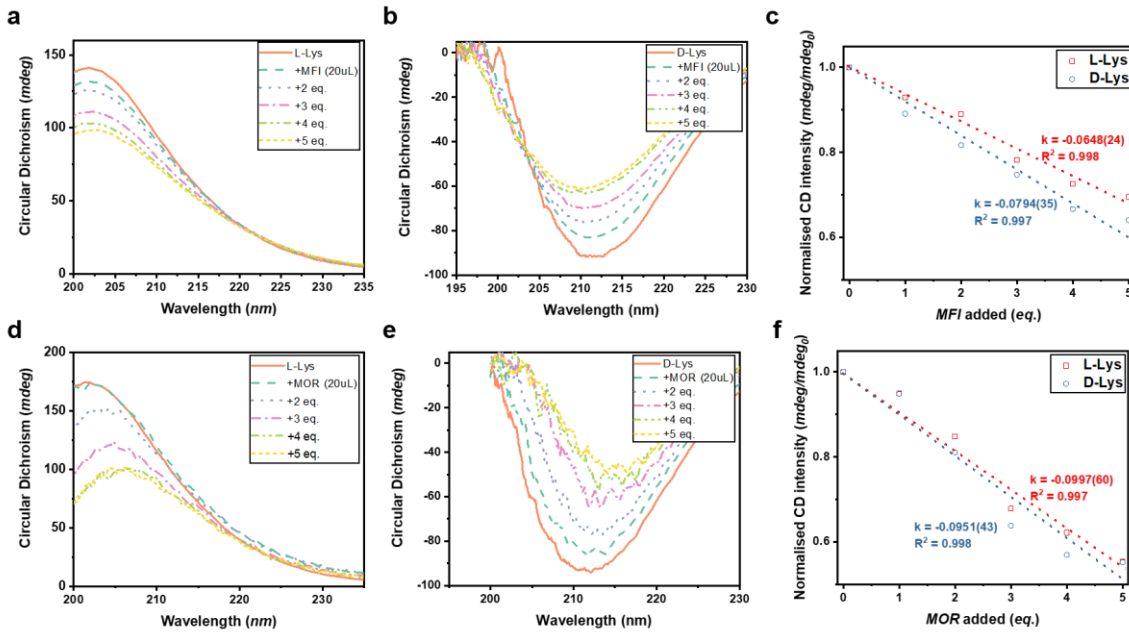


Figure S3. Circular dichroism (CD) spectra of (a) L-Lys and (b) D-Lys in water ($c_{\text{L-lysine}} = 0.01 \text{ mM}$, $c_{\text{D-lysine}} = 0.01 \text{ mM}$), with the successive addition of 20 μL of **MFI** ($c_{\text{H-ZSM-5}} = 140 \text{ g L}^{-1}$). Accumulation of three for averaging at each data point was taken to increase reliability. (c) The comparison of the normalised peak CD intensities ($\text{mdeg}/\text{mdeg}_0$) with respect to the MFI added⁹. (d-f) The corresponding data for L- and D-Lys over **MOR** zeolites. Equal amounts of **MFI** and **MOR** zeolites were added to the L- and D-Lys solutions sequentially. We observed that the CD signal decay rate of L-lysine is lower than that of D-Lys ($k_{\text{L-Lys}} = -0.0648$ vs $k_{\text{D-Lys}} = -0.0794$) upon the addition of **MFI**. In contrast, a similar CD signal decay rate was observed upon the addition of **MOR** to L-Lys and D-Lys solutions ($k_{\text{L-Lys}} = -0.0997$ vs $k_{\text{D-Lys}} = -0.0951$).

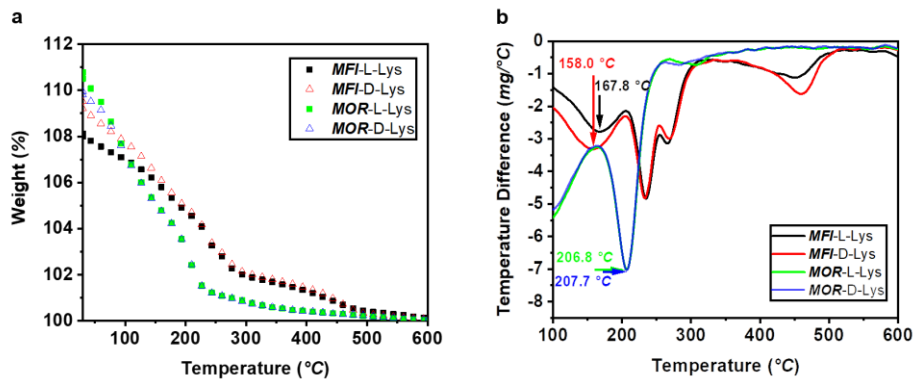


Figure S4. (a) TGA and (b) the corresponding differential curves of **MFI-L-Lys**, **MFI-D-Lys**, **MOR-L-Lys**, and **MOR-D-Lys**.

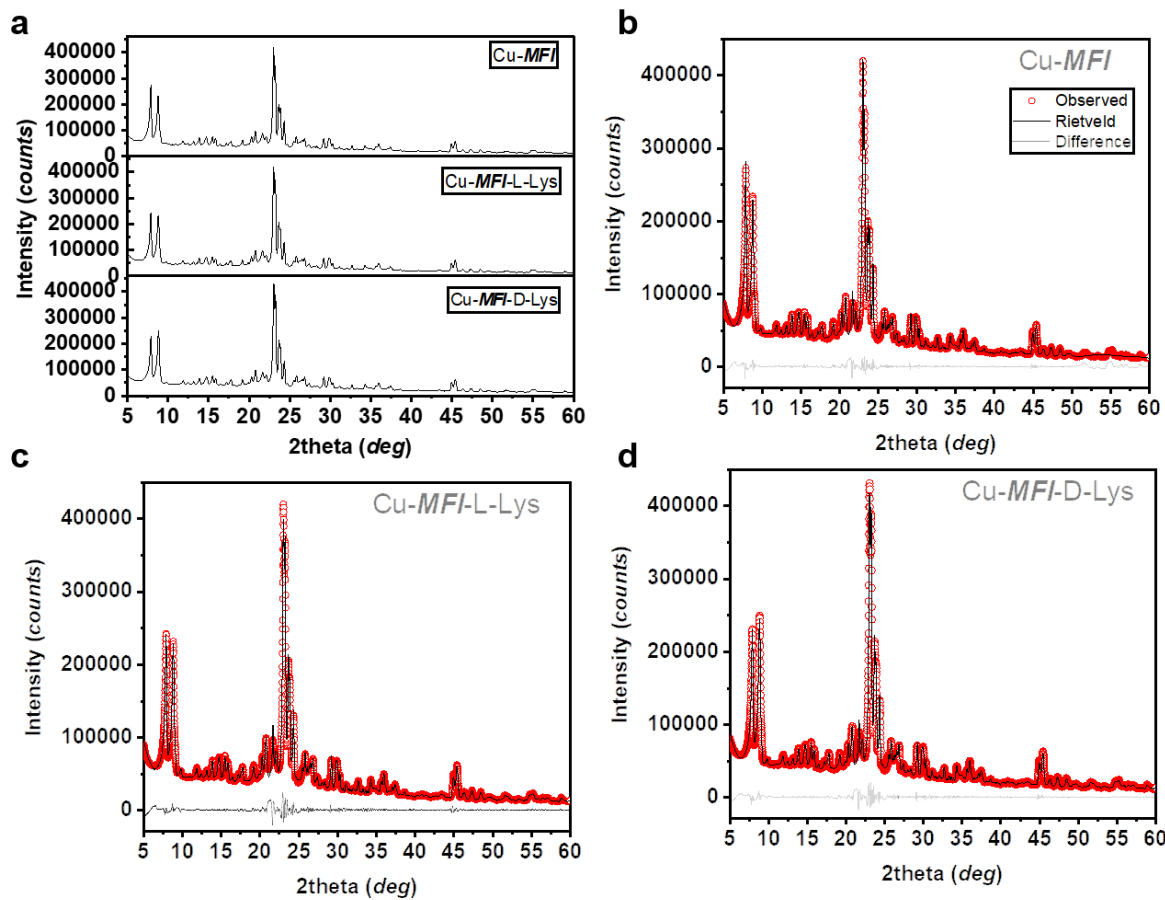


Figure S5. (a) Powder XRD patterns of Cu-**MFI**, Cu-**MFI**-L-Lys and Cu-**MFI**-D-Lys, (b-d) The corresponding Rietveld refinements of Cu-**MFI**, Cu-**MFI**-L-Lys and Cu-**MFI**-D-Lys. The structural parameters are summarised in Table S5.

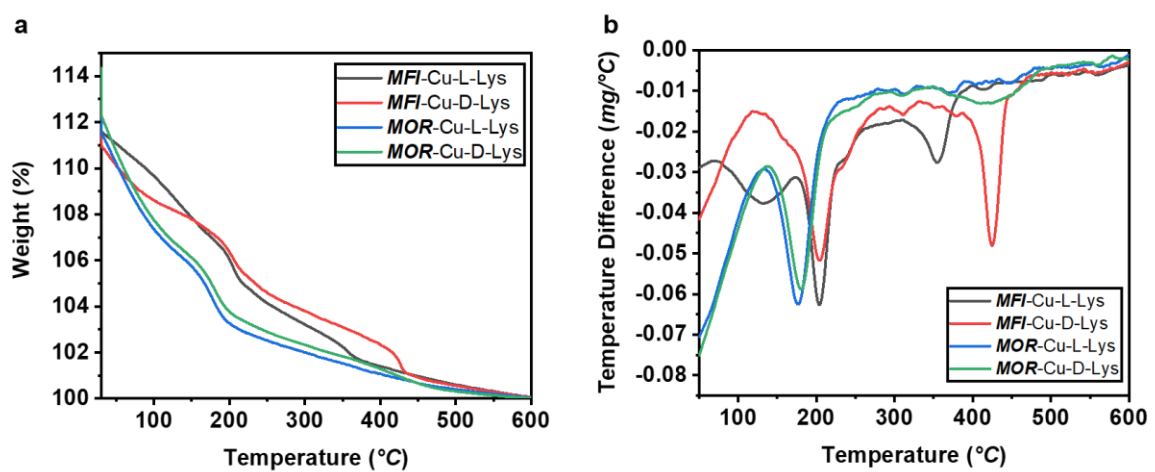


Figure S6. (a) TGA and (b) the corresponding differential curves of Cu-**MFI**-L-Lys, Cu-**MFI**-D-Lys, Cu-**MOR**-L-Lys, and Cu-**MOR**-D-Lys.

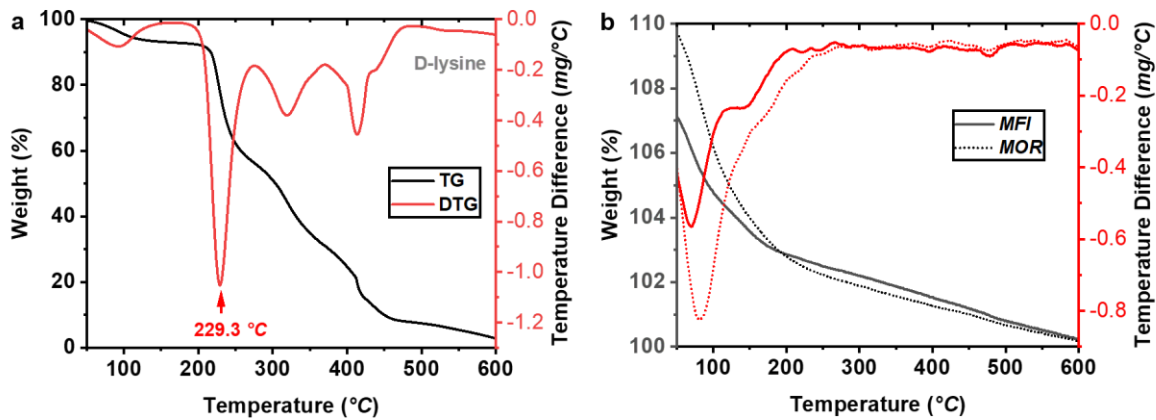


Figure S7. TGA and the corresponding differential curves of (a) pristine D-Lys, and (b) pristine **MFI** and **MOR** zeolites. The TGA curve of L-Lys can be found in various other literature, such as by Martins et al.¹⁰

The TGA measurement of pristine lysine, **MFI** and **MOR** zeolites samples were performed in N₂ (40 mL min⁻¹) up to 600 °C using a thermogravimetric analyser/differential scanning calorimeter (Mettler Toledo TGA/DSC3+). As shown in Figure S6 (a), the largest differential peak of pristine D-lysine is observed at 229.3 °C (that agrees with the decomposition value of 224 °C as reported in database/literature¹¹). However, based on our TGA studies of D/L-Lys from **MFI** and **MOR**, the main desorption features are observed at temperatures below the decomposition temperatures of 224-229 °C. Our discussion based on the peak desorption temperatures at lower temperature range should not be affected by the decomposition process. Also, as seen in Figure S6 (b), the desorption behaviour in zeolites is mainly the desorption of free water and bound water molecules, where a significant proportion of weight is lost below 100 °C. Hence, from the TGA profiles of D/L-Lys from **MFI** and **MOR**, it can be assumed that most lysine molecules are desorbed from the BASs of zeolites below the lysine decomposition temperature of 224-229 °C.

Table S1. Crystallographic data from SXRD measurements of ***MFI***-L-Lys, ***MFI***-D-Lys, ***MOR***-L-Lys, and ***MOR***-D-Lys. SXRD data were obtained from BL02B2 at SPring-8 (Japan), $\lambda = 0.689556(2)$ Å and 2θ -zero point = -0.000015(1)°.

	Pristine <i>MFI</i>	<i>MFI</i> -L-Lys	<i>MFI</i> -D-Lys	Pristine <i>MOR</i>	<i>MOR</i> -L-Lys	<i>MOR</i> -D-Lys
Space group	<i>Pnma</i>	<i>Pnma</i>	<i>Pnma</i>	<i>Cmcm</i>	<i>Cmcm</i>	<i>Cmcm</i>
Crystal system	Orthorhombic	Orthorhombic	Orthorhombic	Orthorhombic	Orthorhombic	Orthorhombic
<i>a</i> (Å)	20.11041(20)	20.15190(17)	20.14914(16)	18.11056(21)	18.10779(19)	18.10043(17)
<i>b</i> (Å)	19.92073(21)	19.94330(18)	19.94016(17)	20.32304(20)	20.34649(19)	20.33833(17)
<i>c</i> (Å)	13.41659(17)	13.43695(15)	13.43401(14)	7.47910(7)	7.484290(7)	7.482153(7)
<i>V</i> (Å ³)	5374.87(10)	5400.248(89)	5397.478(86)	2752.768(48)	2757.437(47)	2754.425(43)
Number of parameters	28	28	28	26	26	26
Number of <i>hkl</i> s	1321	1321	1321	853	853	853
<i>R</i> _{wp} / <i>R</i> _{exp} / <i>R</i> _p (%)	12.633/1.146/8.001	11.102/1.062/6.209	10.047/1.122/5.843	10.002/1.172/6.130	10.503/1.102/6.402	9.200/1.265/5.509

*R*_{wp}: weighted profile; *R*_{exp}: expected; *R*_p: profile.

Table S2(a). Atomic parameters derived from the SXRD measurements of **MFI-L-Lys** ($\text{SiO}_2:\text{Al}_2\text{O}_3 = 46$), measured at 25 °C.

Species	Atom	x	y	z	SOF	$B_{\text{eq}} (\text{\AA}^2)$	Wyckoff
Zeolite framework	O1	0.3800(19)	0.052(2)	0.762(3)	1	1.73(16)	8d
	O2	0.300(2)	0.053(2)	0.930(2)	1	1.73(16)	8d
	O3	0.197(2)	0.0687(15)	0.032(2)	1	1.73(16)	8d
	O4	0.0977(17)	0.060(2)	0.909(3)	1	1.73(16)	8d
	O5	0.116(2)	0.050(3)	0.736(3)	1	1.73(16)	8d
	O6	0.2495(19)	0.043(3)	0.749(3)	1	1.73(16)	8d
	O7	0.376(2)	0.837(2)	0.772(3)	1	1.73(16)	8d
	O8	0.311(2)	0.8467(17)	0.925(3)	1	1.73(16)	8d
	O9	0.198(2)	0.8502(14)	0.024(2)	1	1.73(16)	8d
	O10	0.0797(18)	0.8390(18)	0.928(3)	1	1.73(16)	8d
	O11	0.119(2)	0.840(2)	0.742(3)	1	1.73(16)	8d
	O12	0.242(2)	0.838(2)	0.765(3)	1	1.73(16)	8d
	O13	0.3186(17)	0.9445(19)	0.820(2)	1	1.73(16)	8d
	O14	0.0843(16)	0.954(2)	0.808(2)	1	1.73(16)	8d
	O15	0.417(2)	0.126(2)	0.608(3)	1	1.73(16)	8d
	O16	0.4130(19)	0.9879(18)	0.582(3)	1	1.73(16)	8d
	O17	0.3962(19)	0.8574(18)	0.584(3)	1	1.73(16)	8d
	O18	0.191(2)	0.1248(18)	0.618(2)	1	1.73(16)	8d
	O19	0.208(2)	0.0087(19)	0.608(3)	1	1.73(16)	8d
	O20	0.210(2)	0.876(2)	0.585(2)	1	1.73(16)	8d
	O21	1.006(2)	0.055(2)	0.798(2)	1	1.73(16)	8d
	O22	0.9906(19)	0.849(2)	0.803(3)	1	1.73(16)	8d
	O23	0.426(3)	0.75	0.652(4)	1	1.73(16)	4c
	O24	0.197(3)	0.75	0.663(3)	1	1.73(16)	4c
	O25	0.280(2)	0.75	0.052(4)	1	1.73(16)	4c
	O26	0.095(3)	0.75	0.070(4)	1	1.73(16)	4c
Si1	0.4204(10)	0.0579(12)	0.6627(14)	1	0.87(8)	8d	
Si2	0.3106(13)	0.0307(9)	0.8245(15)	1	0.87(8)	8d	
Si3	0.2734(9)	0.0569(11)	0.0372(14)	1	0.87(8)	8d	
Si4	0.1164(10)	0.0685(10)	0.0397(16)	1	0.87(8)	8d	
Si5	0.0735(10)	0.0274(10)	0.8120(16)	1	0.87(8)	8d	
Si6	0.1847(10)	0.0540(11)	0.6809(14)	1	0.87(8)	8d	
Si7	0.4232(10)	0.8255(10)	0.6659(16)	1	0.87(8)	8d	
Si8	0.3115(12)	0.8700(9)	0.8166(14)	1	0.87(8)	8d	
Si9	0.2791(9)	0.8246(9)	0.0291(16)	1	0.87(8)	8d	

	Si10	0.1193(11)	0.8287(10)	0.0431(16)	1	0.87(8)	8d
	Si11	0.0693(11)	0.8770(10)	0.8181(16)	1	0.87(8)	8d
	Si12	0.1878(12)	0.8234(9)	0.6848(15)	1	0.87(8)	8d
L-Lys1	C7	-2.020(2)	0.668(2)	1.512(3)	0.459(9)	10	4c
	C6	-1.959(5)	0.623(6)	1.499(5)	0.459(9)	10	4c
	C5	-1.914(5)	0.642(9)	1.414(7)	0.459(9)	10	4c
	N10	-1.995(10)	0.559(3)	1.476(8)	0.459(9)	10	4c
	C4	-1.900(9)	0.719(11)	1.400(13)	0.459(9)	10	4c
	C3	-1.841(11)	0.731(16)	1.330(18)	0.459(9)	10	4c
	C2	-1.778(8)	0.69(3)	1.37(3)	0.459(9)	10	4c
	N1	-1.752(15)	0.73(4)	1.44(3)	0.459(9)	10	4c
	O8	-2.056(3)	0.651(4)	1.594(4)	0.459(9)	10	4c
	O9	-2.029(6)	0.727(3)	1.531(5)	0.459(9)	10	4c
L-Lys2	C7	-0.620(2)	0.762(3)	1.262(3)	0.440(8)	10	4c
	C6	-0.545(3)	0.77(2)	1.245(5)	0.440(8)	10	4c
	C5	-0.525(6)	0.79(3)	1.139(6)	0.440(8)	10	4c
	N10	-0.522(15)	0.71(3)	1.278(6)	0.440(8)	10	4c
	C4	-0.52(3)	0.86(3)	1.106(10)	0.440(8)	10	4c
	C3	-0.51(3)	0.87(3)	0.993(10)	0.440(8)	10	4c
	C2	-0.49(5)	0.94(4)	0.964(18)	0.440(8)	10	4c
	N1	-0.55(6)	0.98(3)	0.94(3)	0.440(8)	10	4c
	O8	-0.635(3)	0.755(7)	1.360(3)	0.440(8)	10	4c
	O9	-0.669(9)	0.796(14)	1.251(4)	0.440(8)	10	4c

Table S2(b). Atomic parameters derived from the SXRD measurements of **MFI-D-Lys** ($\text{SiO}_2:\text{Al}_2\text{O}_3 = 46$), measured at 25 °C.

Species	Atom	x	y	z	SOF	$B_{\text{eq}} (\text{\AA}^2)$	Wyckoff
Zeolite framework	O1	0.3866(19)	0.050(2)	0.750(2)	1	1.56(16)	8d
	O2	0.312(2)	0.053(2)	0.919(2)	1	1.56(16)	8d
	O3	0.193(2)	0.0644(18)	0.032(2)	1	1.56(16)	8d
	O4	0.1058(16)	0.059(2)	0.944(3)	1	1.56(16)	8d
	O5	0.109(2)	0.041(2)	0.729(3)	1	1.56(16)	8d
	O6	0.2533(19)	0.054(3)	0.762(3)	1	1.56(16)	8d
	O7	0.375(2)	0.842(2)	0.801(3)	1	1.56(16)	8d
	O8	0.310(2)	0.8511(18)	0.930(3)	1	1.56(16)	8d
	O9	0.189(2)	0.8478(14)	0.025(2)	1	1.56(16)	8d
	O10	0.087(2)	0.8356(19)	0.927(3)	1	1.56(16)	8d
	O11	0.126(2)	0.840(2)	0.736(3)	1	1.56(16)	8d
	O12	0.243(2)	0.828(2)	0.759(3)	1	1.56(16)	8d
	O13	0.2923(18)	0.947(2)	0.814(2)	1	1.56(16)	8d
	O14	0.0675(16)	0.951(2)	0.803(3)	1	1.56(16)	8d
	O15	0.411(2)	0.123(2)	0.596(3)	1	1.56(16)	8d
	O16	0.404(2)	1.003(2)	0.577(3)	1	1.56(16)	8d
	O17	0.394(2)	0.865(2)	0.589(3)	1	1.56(16)	8d
	O18	0.197(3)	0.123(2)	0.618(3)	1	1.56(16)	8d
	O19	0.411(2)	0.123(2)	0.596(3)	1	1.56(16)	8d
	O20	0.404(2)	1.003(2)	0.577(3)	1	1.56(16)	8d
	O21	0.394(2)	0.865(2)	0.589(3)	1	1.56(16)	8d
	O22	0.197(3)	0.123(2)	0.618(3)	1	1.56(16)	8d
	O23	0.429(3)	0.75	0.643(4)	1	1.56(16)	4c
	O24	0.196(3)	0.75	0.665(4)	1	1.56(16)	4c
	O25	0.288(3)	0.75	0.074(4)	1	1.56(16)	4c
	O26	0.111(3)	0.75	0.054(4)	1	1.56(16)	4c
Si1	0.4242(10)	0.0541(13)	0.6586(14)	1	0.78(8)	8d	
Si2	0.3046(12)	0.0318(9)	0.8217(14)	1	0.78(8)	8d	
Si3	0.2766(9)	0.0556(13)	0.0320(15)	1	0.78(8)	8d	
Si4	0.1176(11)	0.0659(11)	0.0452(15)	1	0.78(8)	8d	
Si5	0.0720(10)	0.0304(10)	0.8190(17)	1	0.78(8)	8d	
Si6	0.1861(11)	0.0557(11)	0.6809(13)	1	0.78(8)	8d	
Si7	0.4254(11)	0.8235(10)	0.6761(17)	1	0.78(8)	8d	
Si8	0.3064(13)	0.8771(9)	0.8156(15)	1	0.78(8)	8d	
Si9	0.2782(10)	0.8274(10)	0.0372(17)	1	0.78(8)	8d	

	Si10	0.1211(11)	0.8250(11)	0.0341(17)	1	0.78(8)	8d
	Si11	0.0670(11)	0.8674(11)	0.8081(16)	1	0.78(8)	8d
	Si12	0.1936(13)	0.8250(9)	0.6831(16)	1	0.78(8)	8d
D-Lys1	C7	-2.036(2)	0.638(2)	1.507(3)	0.508(10)	10	4c
	C6	-1.990(3)	0.579(3)	1.483(5)	0.508(10)	10	4c
	C5	-1.914(3)	0.597(4)	1.465(9)	0.508(10)	10	4c
	N10	-1.997(4)	0.536(3)	1.573(7)	0.508(10)	10	4c
	C4	-1.908(3)	0.669(6)	1.43(2)	0.508(10)	10	4c
	C3	-1.832(4)	0.682(8)	1.41(3)	0.508(10)	10	4c
	C2	-1.820(7)	0.746(14)	1.36(5)	0.508(10)	10	4c
	N1	-1.763(17)	0.74(3)	1.28(5)	0.508(10)	10	4c
	O8	-2.092(2)	0.621(3)	1.545(5)	0.508(10)	10	4c
	O9	-2.022(3)	0.683(3)	1.563(4)	0.508(10)	10	4c
D-Lys2	C7	-0.589(3)	0.724(6)	1.329(4)	0.371(8)	10	4c
	C6	-0.528(5)	0.742(14)	1.266(6)	0.371(8)	10	4c
	C5	-0.536(7)	0.734(16)	1.150(5)	0.371(8)	10	4c
	N10	-0.469(7)	0.72(3)	1.102(10)	0.371(8)	10	4c
	C4	-0.432(17)	0.79(4)	1.10(2)	0.371(8)	10	4c
	C3	-0.47(3)	0.84(3)	1.04(4)	0.371(8)	10	4c
	C2	-0.50(4)	0.89(2)	1.12(6)	0.371(8)	10	4c
	N1	-0.589(5)	0.747(7)	1.419(5)	0.371(8)	10	4c
	O8	-0.646(4)	0.739(11)	1.306(6)	0.371(8)	10	4c
	O9	-0.518(16)	0.814(15)	1.292(9)	0.371(8)	10	4c

Table S2(c). Atomic parameters derived from the SXRD measurements of **MOR-L-Lys** ($\text{SiO}_2:\text{Al}_2\text{O}_3 = 25$), measured at 25 °C.

Species	Atom	x	y	z	SOF	$B_{\text{eq}} (\text{\AA}^2)$	Wyckoff
Zeolite framework	O1	0.2814(10)	0	0	1	1.53(12)	8e
	O2	0.3296(10)	0.0849(9)	0.25	1	1.53(12)	8g
	O3	0.3790(7)	0.0907(7)	0.9408(17)	1	1.53(12)	16h
	O4	0.2358(7)	0.1220(7)	0.9905(16)	1	1.53(12)	16h
	O5	0.3289(8)	0.3098(12)	0.25	1	1.53(12)	8g
	O6	0.25	0.25	0	1	1.53(12)	8d
	O7	0.3715(6)	0.3033(9)	0.9209(15)	1	1.53(12)	16h
	O8	0	0.3991(13)	0.25	1	1.53(12)	4c
	O9	0.0959(7)	0.3016(10)	0.25	1	1.53(12)	8g
	O10	0	0.1939(18)	0.25	1	1.53(12)	4c
L-Lys1	Si1	0.3063(4)	0.0732(3)	0.0369(9)	1	0.77(6)	16h
	Si2	0.3033(3)	0.3113(4)	0.0432(7)	1	0.77(6)	16h
	Si3	0.0889(5)	0.3810(5)	0.25	1	0.77(6)	8g
	Si4	0.0815(5)	0.2259(4)	0.25	1	0.77(6)	8g
	C7	-0.6558(14)	0.6990(18)	0.961(4)	0.211(4)	10	16h
	C6	-0.5711(14)	0.703(3)	0.961(6)	0.211(4)	10	16h
	C5	-0.5383(17)	0.745(4)	0.816(7)	0.211(4)	10	16h
	N10	-0.555(3)	0.633(3)	0.929(6)	0.211(4)	10	16h
	C4	-0.562(4)	0.820(3)	0.814(7)	0.211(4)	10	16h
	C3	-0.536(4)	0.854(4)	0.643(8)	0.211(4)	10	16h
O8	C2	-0.551(7)	0.930(4)	0.652(10)	0.211(4)	10	16h
	N1	-0.541(6)	0.951(4)	0.469(10)	0.211(4)	10	16h
	O9	-0.6815(16)	0.665(2)	1.103(4)	0.211(4)	10	16h
	O9	-0.706(2)	0.738(2)	0.980(5)	0.211(4)	10	16h

Table S2(d). Atomic parameters derived from the SXRD measurements of **MOR-D-Lys** ($\text{SiO}_2:\text{Al}_2\text{O}_3 = 25$), measured at 25 °C.

Species	Atom	x	y	z	SOF	$B_{\text{eq}} (\text{\AA}^2)$	Wyckoff
Zeolite framework	O1	0.2728(11)	0	0	1	1.53(12)	8e
	O2	0.3333(11)	0.0800(9)	0.25	1	1.53(12)	8g
	O3	0.3777(8)	0.0894(6)	0.9298(16)	1	1.53(12)	16h
	O4	0.2303(7)	0.1275(6)	0.9987(16)	1	1.53(12)	16h
	O5	0.3291(9)	0.3081(12)	0.25	1	1.53(12)	8g
	O6	0.25	0.25	0	1	1.53(12)	8d
	O7	0.3686(6)	0.3068(8)	0.9266(15)	1	1.53(12)	16h
	O8	0	0.4041(14)	0.25	1	1.53(12)	4c
	O9	0.0932(7)	0.3011(10)	0.25	1	1.53(12)	8g
	O10	0	0.1979(18)	0.25	1	1.53(12)	4c
D-Lys1	Si1	0.3041(4)	0.0744(3)	0.0337(8)	1	0.77(6)	16h
	Si2	0.3045(3)	0.3094(4)	0.0411(7)	1	0.77(6)	16h
	Si3	0.0863(5)	0.3820(5)	0.25	1	0.77(6)	8g
	Si4	0.0863(5)	0.2246(4)	0.25	1	0.77(6)	8g
	LC7	-0.546(3)	0.6364(18)	0.849(7)	0.140(2)	10	16h
	LC6	-0.541(12)	0.5623(19)	0.810(8)	0.140(2)	10	16h
	LC5	-0.543(16)	0.541(2)	0.607(8)	0.140(2)	10	16h
	LN10	-0.608(16)	0.536(8)	0.904(9)	0.140(2)	10	16h
	LC4	-0.472(13)	0.563(10)	0.514(8)	0.140(2)	10	16h
	LC3	-0.481(17)	0.545(9)	0.313(8)	0.140(2)	10	16h
D-Lys2	LC2	-0.408(18)	0.544(18)	0.219(10)	0.140(2)	10	16h
	LN1	-0.42(2)	0.520(17)	0.028(10)	0.140(2)	10	16h
	LO8	-0.527(4)	0.654(3)	1.007(7)	0.140(2)	10	16h
	LO9	-0.513(7)	0.678(5)	0.763(7)	0.140(2)	10	16h

Table S3(a). Summary of the structural parameters from the Rietveld refinements of the in-situ SXRD measurements of **MFI-L-Lys**.

Environmental Temperature (°C)	R _{wp} (%)	R _{exp} (%)	Lattice parameter <i>a</i> (Å)	Lattice parameter <i>b</i> (Å)	Lattice parameter <i>c</i> (Å)	Unit cell volume (Å ³)
25	12.5483	1.3825	20.15453	19.94753	13.43991	5403.288
50	12.0483	1.3859	20.1565	19.95226	13.44095	5405.516
75	12.0654	1.3827	20.15553	19.95456	13.44019	5405.576
100	12.263	1.3797	20.15353	19.95617	13.43917	5405.064
125	12.5359	1.3777	20.15063	19.95724	13.43806	5404.131
150	12.9972	1.3744	20.14746	19.95786	13.43716	5403.084
175	13.5077	1.3719	20.14327	19.95878	13.43659	5401.981
200	13.55	1.3666	20.13765	19.9595	13.43551	5400.234
225	13.7388	1.3654	20.13465	19.95885	13.43397	5398.636
250	13.9929	1.3619	20.13382	19.95845	13.43435	5398.456
275	14.1585	1.3622	20.13446	19.95729	13.43262	5397.620
300	14.3031	1.3591	20.13282	19.95483	13.43145	5396.044
325	14.3343	1.3542	20.13039	19.95275	13.43031	5394.372
350	14.4304	1.3524	20.12777	19.9509	13.42914	5392.702
375	14.317	1.3466	20.12576	19.95008	13.42793	5391.455
400	14.3966	1.3447	20.12408	19.94998	13.42753	5390.818
425	14.408	1.342	20.12275	19.95055	13.42752	5390.611
450	14.4804	1.3378	20.12100	19.95157	13.42794	5390.585
475	14.6643	1.3334	20.11915	19.95318	13.42904	5390.969
500	14.6876	1.3333	20.11803	19.95436	13.42974	5391.266

Table S3(b). Summary of the structural parameters from the Rietveld refinements of the in-situ SXRD measurements of **MFI-D-Lys**.

Environmental Temperature (°C)	R _{wp} (%)	R _{exp} (%)	Lattice parameter a (Å)	Lattice parameter b (Å)	Lattice parameter c (Å)	Unit cell volume (Å ³)
25	12.7336	1.4712	20.15659	19.94892	13.44054	5404.469
50	12.3758	1.4775	20.15756	19.95326	13.44177	5406.403
75	12.3559	1.472	20.15643	19.95532	13.44058	5406.177
100	12.4771	1.4699	20.15407	19.95658	13.43924	5405.346
125	12.7712	1.4674	20.15117	19.95759	13.43824	5404.443
150	13.2733	1.4663	20.14850	19.95839	13.43778	5403.758
175	13.7516	1.461	20.14503	19.95929	13.43693	5402.731
200	13.7797	1.4579	20.13956	19.96009	13.43605	5401.122
225	13.8672	1.4553	20.13565	19.95928	13.43446	5399.217
250	14.1866	1.4462	20.13216	19.95726	13.43299	5397.147
275	14.2233	1.4501	20.12965	19.95884	13.43427	5397.413
300	14.2259	1.4481	20.12575	19.95991	13.43479	5396.866
325	14.3474	1.4451	20.12057	19.96126	13.43479	5395.841
350	14.3559	1.4447	20.11409	19.96357	13.43518	5394.886
375	14.3808	1.4426	20.10743	19.96667	13.43636	5394.410
400	14.2996	1.4424	20.09948	19.97005	13.43798	5393.840
425	14.3068	1.4406	20.09388	19.97262	13.43931	5393.564
450	14.3075	1.4387	20.09024	19.97427	13.44011	5393.357
475	14.3053	1.4364	20.08874	19.97451	13.44055	5393.194
500	14.3567	1.4379	20.08840	19.97392	13.44079	5393.040

Table S4(a). Summary of the structural parameters from the Rietveld refinements of the *in-situ* SXRD measurements of **MFI-L-Lys**. The estimated standard deviation of all the SOF values are less than 1%.

Environmental Temperature (°C)	Site Occupancy Factor of Site I	Site Occupancy Factor of Site II
25	0.4409	0.3886
50	0.4353	0.3833
75	0.4213	0.3655
100	0.3984	0.3447
125	0.3686	0.3213
150	0.3263	0.3044
175	0.2894	0.2913
200	0.2524	0.282
225	0.2225	0.261
250	0.1833	0.224
275	0.1973	0.2179
300	0.1856	0.1905
325	0.1489	0.1691
350	0.1181	0.1433
375	0.1137	0.1285
400	0.0977	0.1084
425	0.0884	0.0873
450	0.0755	0.0735
475	0.0228	0.069
500	0.0134	0.0586

Table S4(b). Summary of the structural parameters from the Rietveld refinements of the *in-situ* SXRD measurements of **MFI-D-Lys**. The estimated standard deviation of all the SOF values are less than 1%.

Environmental Temperature (°C)	Site Occupancy Factor of Site I	Site Occupancy Factor of Site II
25	0.4253	0.4128
50	0.4207	0.4061
75	0.4025	0.3959
100	0.3847	0.3769
125	0.3598	0.352
150	0.3338	0.3295
175	0.3063	0.2984
200	0.2811	0.2703
225	0.2545	0.242
250	0.2023	0.1983
275	0.2069	0.18
300	0.2069	0.1721
325	0.1954	0.1622
350	0.188	0.1538
375	0.1828	0.1445
400	0.1806	0.1282
425	0.1798	0.1121
450	0.1738	0.109
475	0.1651	0.1051
500	0.1605	0.0954

Table S5. Crystallographic data of the PXRD measurements of Cu-**MFI**, Cu-**MFI-L-Lys**, Cu-**MFI-D-Lys**. PXRD data were obtained from Rigaku SmartLab 9kW, $\lambda=1.5406(1)$ Å.

	Cu- MFI	Cu- MFI-L-Lys	Cu- MFI-D-Lys
X-ray energy (keV)	8.0478	8.0478	8.0478
X-ray Diffractometer	Rigaku SmartLab 9kW	Rigaku SmartLab 9kW	Rigaku SmartLab 9kW
Wavelength (Å)	1.5406(1)	1.5406(1)	1.5406(1)
2θ - zero point (°)	0.02084(17)	0.01599(26)	0.03620(13)
Space group	<i>Pnma</i>	<i>Pnma</i>	<i>Pnma</i>
Crystal system	Orthorhombic	Orthorhombic	Orthorhombic
<i>a</i> (Å)	20.15257(18)	20.16519(58)	20.15781(37)
<i>b</i> (Å)	19.95598(19)	19.94345(32)	19.94297(18)
<i>c</i> (Å)	13.45167(19)	13.44958(15)	13.44905(2)
<i>V</i> (Å ³)	5409.768(70)	5408.936(23)	5406.610(40)
2θ range for refinement (°)	2-60	2-60	2-60
Number of parameters	28	28	28
Number of <i>hkl</i> s	840	840	840
Refinement methods	Le Bail	Le Bail	Le Bail
<i>R</i> _{wp} / <i>R</i> _{exp} / <i>R</i> _p (%)	9.619/0.428/5.040	9.422/0.426/4.922	8.775/ 0.433/4.589

*R*_{wp}: weighted profile; *R*_{exp}: expected; *R*_p: profile.

References:

- 1 S. Kawaguchi, M. Takemoto, K. Osaka, E. Nishibori, C. Moriyoshi, Y. Kubota, Y. Kuroiwa and K. Sugimoto, High-throughput powder diffraction measurement system consisting of multiple MYTHEN detectors at beamline BL02B2 of SPring-8, *Rev. Sci. Instrum.*, , DOI:10.1063/1.4999454.
- 2 N. H. Heo, C. W. Kim, H. J. Kwon, G. H. Kim, S. H. Kim, S. B. Hong and K. Seff, Detailed determination of the Ti⁺ positions in zeolite Ti-ZSM-5. Single-crystal structures of fully dehydrated Ti-ZSM-5 and H-ZSM-5 (MFI, Si/Al = 29). Additional evidence for a nonrandom distribution of framework aluminum, *J. Phys. Chem. C*, 2009, **113**, 19937–19956.
- 3 P. Thompson, D. E. Cox and J. B. Hastings, Rietveld refinement of Debye–Scherrer synchrotron X-ray data from Al₂O₃, *J. Appl. Crystallogr.*, 1987, **20**, 79–83.
- 4 D. Watkin, Uequiv: its past, present and future, *Acta Crystallogr. Sect. B Struct. Sci.*, 2000, **56**, 747–749.
- 5 R. I. Cooper, A. L. Thompson and D. J. Watkin, CRYSTALS enhancements: Dealing with hydrogen atoms in refinement, *J. Appl. Crystallogr.*, 2010, **43**, 1100–1107.
- 6 H. Van Koningsveld, High - temperature (350 K) orthorhombic framework structure of zeolite H - ZSM - 5, *Acta Crystallogr. Sect. B*, 1990, **46**, 731–735.
- 7 B. F. Mentzen, Characterization of guest molecules adsorbed on zeolites of known structure by combined X-ray powder profile refinements and conventional difference-Fourier techniques. Part I - Localization of the benzene molecule in a pentasil type zeolite, *Mater. Res. Bull.*, 1987, **22**, 337–343.
- 8 R. Goyal, A. N. Fitch and H. Jobic, Powder Neutron and X-ray Diffraction Studies of Benzene Adsorbed in Zeolite ZSM-5, *J. Phys. Chem. B*, 2000, **104**, 2878–2884.
- 9 T. Chen, B. Huang, S. Day, C. C. Tang, S. C. E. Tsang, K. Wong and T. W. B. Lo, Differential adsorption of L - and D - lysine on achiral MFI zeolites as determined by synchrotron X - ray powder diffraction and thermogravimetric analysis, *Angew. Chemie*, 2019, ange.201909352.
- 10 T. da S. Martins, J. do R. Matos, G. Vicentini and P. C. Isolani, Synthesis, characterization, spectroscopy and thermal analysis of rare earth picrate complexes with L-lysine, *J. Therm. Anal. Calorim.*, 2005, **82**, 77–82.
- 11 D. R. Lide, DR 2007-2008, *Handb. Chem. Physics*, 88th Ed, CRC Press.